Power Losses of Three Phase Rectifier Topologies in Small Wind Turbines

Kristina Buchert, Friedrich W. Fuchs
University of Kiel, Chair for Power Electronics
Kaiserstrasse 2, 24143 Kiel, Germany
Email: krb@tf.uni-kiel.de, fwf@tf.uni-kiel.de

Abstract

This paper presents the loss calculation of five different rectifier topologies applied to a small wind turbine system. The diode rectifier, the diode rectifier with a combination of a boost converter or switch mode rectifier as well as a half bridge switch mode rectifier and the two-level converter are considered in this paper. An important factor for a high efficient energy production is the wind speed. For small wind turbines it is rather low and gusty. The aim of this paper is the comparison of the rectifiers regarding the efficiency and the losses for certain wind speeds. Depended on the wind speed, the losses of the converter and the machine of these five rectifiers applied in a small wind turbine are calculated and simulated. Finally, a selection guideline is given for different wind characteristics.

1 Introduction

Small wind turbines (SWT) are specified with a maximum power of 100 kW and a hub height less than 20 m according to the IEC-Standard 61400-2. Typically, a drive train with a permanent magnet synchronous generator (PMSG) including a diode rectifier (DR) combined with a two-level grid side inverter is used for SWT [1, 2]. The costs of this rectifier are low due to the simple construction. Nevertheless, this system leads to a low overall efficiency because it is not able to adapt the generator speed to the maximum power point of the power curve of the generator system. Other rectifier topologies like the boost converter (DRBC) [3], the switch mode rectifier (DRSMR) [4, 5], the half bridge switch mode rectifier(HSMR) [6, 7] and the two-level converter (2LC) [8], therefore become more interesting because they are able to operate in the maximum power point [7–11]. In contrast to the literature, this paper

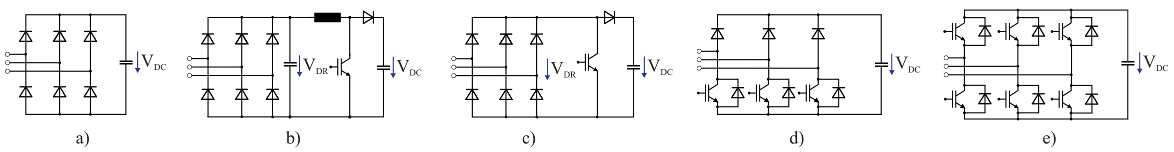

Fig. 1: Investigated rectifier topologies using a PMSG: a) DR, b) DRBC, c) DRSMR, d) HSMR, e) 2LC

considers different wind speeds to calculate the efficiency dependent on the wind speed [7, 9, 10]. Additionally, the power losses of the HSMR are analyzed explicitly.

In section 2 the machine parameters and data of the power semiconductors for the considered 10 kVA system are described. In the third section, the theoretical loss calculation of the rectifiers and the machine is done. The voltage and current functions are presented for each rectifier topology, which is needed for the switching and conduction losses of the power semiconductors. In the forth section the simulation results for certain power semiconductors are shown. At the end, a discussion of the optimal rectifier regarding the efficiency is done.

2 Specifications

In the following tables, the machine parameters as well as the power semiconductors used for the loss calculation are shown. Here only one pair of power semiconductors are considered. To do a comparison, the same power semiconductors are used. The machine used for this investigation is a surface mounted PMSG.

3 Loss Calculation

For the loss calculation the general formulas of the switching and conduction losses of the power semiconductors are shown in this section. The shape of the current through a device is the important in-

ISBN 978-3-8007-3924-0

Tab. 1: Machine parameters for a SPMSM used for SWT system

Parameter	Values
Stator inductance L_S	$18.9\,\mathrm{mH}$
Inertia J	$0.053\,\mathrm{kgm}^2$
Magnetic Flux ϕ	$0.694\,\mathrm{mVs}$
Stator resistance R_{Phase}	$1.2\,\Omega$
Rated speed n_N	$600\,\mathrm{min}^{-1}$
Rated voltage U_N	$426\,\mathrm{V}$
Rated current I_N	$15.79\,\mathrm{A}$
Power factor $\cos(\varphi)$	1

Tab. 2: Used power semiconductors for the rectifiers from *Infineon AG*

Converter	Diode	IGBT
DR	*DDB6U25N16VR*	-
DRBC	*DDB6U25N16VR*	*IKW25N120*
SMR	*DDB6U25N16VR*	*IKW25N120*
HSMR	*DDB6U25N16VR*	*IKW25N120*
2LC	-	*IKW25N120*

fluence factor, which has to be derived for each topology. It is considered that the duty cycle and the modulation factor are constant within each wind speed.

3.1 General formulas for power semiconductor losses

The losses for a power semiconductor are divided into blocking, conduction, switching and driving losses. In the following calculations only, the switching and conduction losses are considered. The blocking and driving losses are neglected [12]. The conduction losses are generally dependent on the applied voltages of the IGBT $v_{\mathrm{CE}}(t)$ and of the diode $v_\mathrm{F}(t)$ and the currents of the IGBT $i_\mathrm{c}(t)$ and of the diode $i_\mathrm{F}(t)$ through the device within one periode T [13].

$$P_{\mathrm{cond,D}} = \frac{1}{T}\int v_\mathrm{F}(t)\cdot i_\mathrm{F}(t)\,\mathrm{d}t \qquad P_{\mathrm{cond,IGBT}} = \frac{1}{T}\int v_{\mathrm{CE}}(t)\cdot i_\mathrm{c}(t)\,\mathrm{d}t \tag{1}$$

For the voltages, a linearization with the differential resistance r_F and r_{CE} and the current $i_\mathrm{c}(t)$ and $i_\mathrm{F}(t)$ for different temperatures is done:

$$\text{Diode: } v_\mathrm{F}(t) = V_{\mathrm{F0}} + r_\mathrm{F}\cdot i_\mathrm{F}(t) \qquad \text{Semiconductor: } v_{\mathrm{CE}}(t) = V_{\mathrm{CE0}} + r_{\mathrm{CE}}\cdot i_\mathrm{c}(t) \tag{2}$$

The differential resistance can be calculated as shown below:

$$\text{Diode: } r_\mathrm{F} = r_{\mathrm{F,25^\circ C}} + TC_\mathrm{r}\cdot\left(T_\mathrm{j} - 25^\circ C\right) \qquad \text{Semiconductor: } r_{\mathrm{CE}} = r_{\mathrm{CE,25^\circ C}} + TC_\mathrm{r}\cdot\left(T_\mathrm{j} - 25^\circ C\right). \tag{3}$$

The switching losses are depended on the switching frequency as well as the turn-on and turn-off energy of the device. The influence of the temperature is considered with the temperature coefficient TC_{ESW} and $TC_{ERR}$and can be found in [13]. Considering a constant DC link voltage, the main influence factor is again the current.

The aim of the calculation is to find the current shape, which goes through each semiconductor and which is dependent on the topology. In fig. 2 the shape of the phase currents of the topologies are shown. As it can be seen, the base of the shape is the current of the DR.

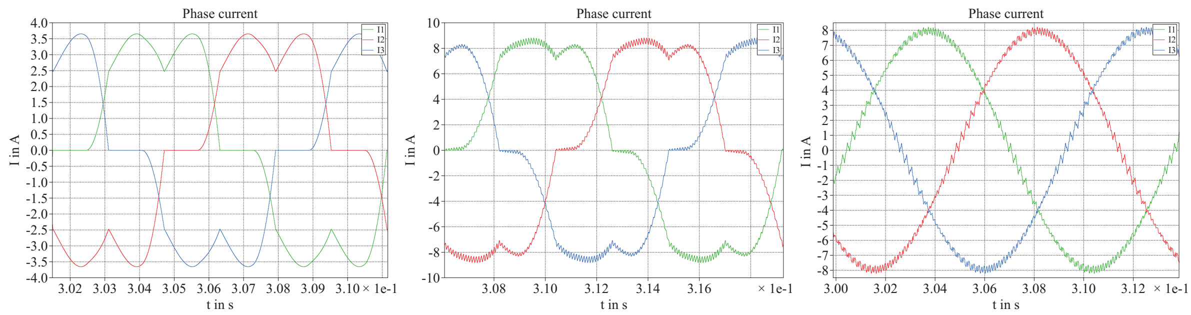

(a) DR (b) DRBC,DRSMR,HSMR (c) 2LC

Fig. 2: Exemplary phase currents of the rectifiers for a wind speed of $v = 8\ m/s$

ISBN 978-3-8007-3924-0

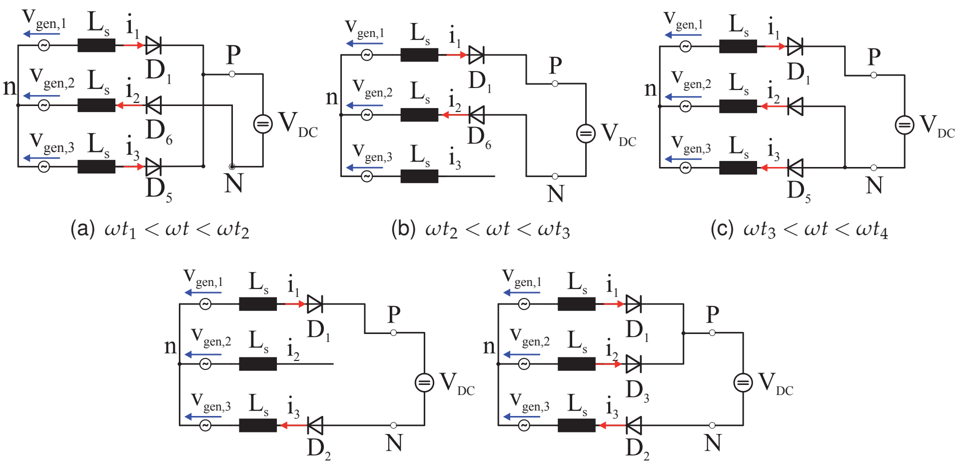

(a) $\omega t_1 < \omega t < \omega t_2$ (b) $\omega t_2 < \omega t < \omega t_3$ (c) $\omega t_3 < \omega t < \omega t_4$

(d) $\omega t_4 < \omega t < \omega t_5$ (e) $\omega t_5 < \omega t < \omega t_6$

Fig. 3: Conduction intervals for calculating the current shape of the positive half cycle the diode rectifier

3.2 Diode Rectifier

For the DR, the switching losses are neglected, because they are low. The shape of the current is an important factor for getting the relevant RMS and mean which are essential for the losses. These currents have to be calculated for different wind speeds [12, 13].

The current of the DR can be calculated out of the conduction intervals, which are shown in fig. 3 (compare to [1, 14, 15]). Applying the Kirchhoffsche law, the differential equations can be derived to eq. 4. $C_1 - C_4$ are the starting points from the interval before.

$$i_{\mathrm{DR}}(\omega t) = \begin{cases} \frac{\hat{V}_{\mathrm{gen}}}{\omega_{\mathrm{gen}} L_s}\left(-\cos(\omega t) + \cos(\omega t_1)\right) + \frac{V_{\mathrm{DC,DR}}}{\omega_{\mathrm{gen}} L_s}\left(-\frac{1}{3}\omega t + \frac{1}{3}\omega t_1\right) & \text{if } \omega t_1 < \omega t < \omega t_2 \\ \frac{\sqrt{3}}{2} \cdot \frac{\hat{V}_{\mathrm{gen}}}{\omega_{\mathrm{gen}} L_s}\left(\sin\left(\omega t - \frac{1}{3}\pi\right) - \sin\left(\omega t_2 - \frac{1}{3}\pi\right)\right) - \frac{1}{2}\frac{V_{\mathrm{DC,DR}}}{\omega_{\mathrm{gen}} L_s}(\omega t - \omega t_2) + C_1 & \text{if } \omega t_2 < \omega t < \omega t_3 \\ \frac{\hat{V}_{\mathrm{gen}}}{\omega_{\mathrm{gen}} L_s}\left(\cos(\omega t_3) - \cos(\omega t)\right) - \frac{2}{3}\frac{V_{\mathrm{DC,DR}}}{\omega_{\mathrm{gen}} L_s}(\omega t - \omega t_3) + C_2 & \text{if } \omega t_3 < \omega t < \omega t_4 \\ -\frac{\sqrt{3}}{2}\frac{\hat{V}_{\mathrm{gen}}}{\omega_{\mathrm{gen}} L_s}\left(\sin\left(\omega t + \frac{1}{3}\pi\right) - \sin\left(\omega t_4 + \frac{1}{3}\pi\right)\right) - \frac{1}{2}\frac{V_{\mathrm{DC,DR}}}{\omega_{\mathrm{gen}} L_s}(\omega t - \omega t_4) + C_3 & \text{if } \omega t_4 < \omega t < \omega t_5 \\ \frac{\hat{V}_{\mathrm{gen}}}{\omega_{\mathrm{gen}} L_s}\left(\cos(\omega t_5) - \cos(\omega t)\right) - \frac{1}{3}\frac{V_{\mathrm{DC,DR}}}{\omega_{\mathrm{gen}} L_s}(\omega t - \omega t_5) + C_4 & \text{if } \omega t_5 < \omega t < \omega t_6 \end{cases} \tag{4}$$

The current is dependent on the generator voltage and speed, which are dependent on the wind speed as it can be seen in the equations below [16]:

$$\left|V_{\mathrm{gen}}\right| = \omega_{\mathrm{gen}} \cdot \Psi_{\mathrm{PM}} \qquad \frac{1}{2T}\rho A v^3 = \omega_{\mathrm{gen}} \tag{5}$$

Combining of eq. (1) - eq. (3) and eq. (4), the overall losses of the DR can be derived to:

$$P_{\mathrm{DR}} = 6 \cdot \left(V_{\mathrm{F0}} \cdot I_{\mathrm{DR,bar}} + \left(r_{\mathrm{F,25^\circ C}} + TC_{\mathrm{r}} \cdot \left(T_{\mathrm{j}} - 25^\circ C\right)\right) \cdot I_{\mathrm{DR,RMS}}^2\right). \tag{6}$$

The mean value and the RMS value can be calculated with the common formulas [17].

3.3 Diode Rectifier with a boost converter

For the loss calculation of the power semiconductors, the influence of the switch of boost converter on the generator phase currents are neglected. First, it does not influence the mean and RMS value and second, it becomes relevant when considering the machine losses. The losses of the diode rectifier part is calculated the similar to the DR but with a lower DC-link voltage. The losses for the inductance are approximated with its inner resistance, which is assumed to be $0.02\ \Omega$ in this analysis.

Assuming a constant switching frequency and a constant DC-link voltage, the DC-link current is the main factor that influences the losses of the boost converter. Therefore, the DC-link current at the output of

ISBN 978-3-8007-3924-0

Tab. 3: Duty cycle operation in dependency on the wind speed for the DRBC, DRSMR and HSMR

wind speed in m/s	1	2	3	4	5	6	7	8	9	10	11
duty cycle	0.80	0.75	0.68	0.62	0.54	0.48	0.42	0.34	0.30	0.27	0.26

the DR has to be calculated, whereas the DC-link voltage is $V_{\mathrm{DC,GR}} = V_{\mathrm{DC}}\,(1-D)$. For the calculation, a constant junction temperature ($T_{\mathrm{j}} = 125\,°\mathrm{C}$) and a constant duty-cycle (Tab. 3) occure for a certain wind speed. The current functions of the diodes and IGBTs for the loss calculation can be summarized as follows:

$$i_{\mathrm{F,DR}}\,(\omega t) = i_{\mathrm{DR}}\,(\omega t, V_{\mathrm{DC,HSS}}) \tag{7}$$

$$i_{\mathrm{F,Diode}}\,(\omega t, D) = i_{\mathrm{DC,DR}}\,(\omega t, V_{\mathrm{DC,HSS}}, D) \tag{8}$$

$$i_{\mathrm{c}}\,(\omega t, D) = i_{\mathrm{DR,DC}}\,(\omega t, D) \tag{9}$$

Finally, with eq. (1) - eq. (3) and eq. (8) - (9), the conduction and switching losses P_{cond} and P_{sw} are:

$$P_{\mathrm{cond,Diode}}(D, T_{\mathrm{j}}, I) = (1-D)\cdot\left(I_{\mathrm{DC,mean}}\cdot(V_{\mathrm{F0}}(T_{\mathrm{j}}) + TC_{\mathrm{v}}\cdot\Delta T_{\mathrm{j}}) + I^2_{\mathrm{DC,mean}}\cdot(r_{\mathrm{F}}(T_{\mathrm{j}}) + TC_{\mathrm{r}}\cdot\Delta T)\right) \tag{10}$$

$$P_{\mathrm{cond,IGBT}}(D, T_{\mathrm{j}}, I) = D\cdot\left(I_{\mathrm{DC,avg}}\cdot(V_{\mathrm{CE0}}(T_{\mathrm{j}}) + TC_{\mathrm{v}}\cdot\Delta T) + I^2_{\mathrm{DC,avg}}\cdot(r_{\mathrm{CE}}(T_{\mathrm{j}}) + TC_{\mathrm{r}}\cdot\Delta T)\right) \tag{11}$$

$$P_{\mathrm{sw,Diode}}(D, T_{\mathrm{j}}, I) = f_{\mathrm{sw}}\cdot E_{\mathrm{rr}}(T_{\mathrm{j}})\cdot\left(\frac{I_{\mathrm{DC,avg}}}{I_{\mathrm{ref}}}\right)^{k_{\mathrm{iD}}}\cdot\left(\frac{V_{\mathrm{DC}}}{V_{\mathrm{ref}}}\right)^{k_{\mathrm{vD}}}\cdot(1 + TC_{\mathrm{Err}}\cdot\Delta T) \tag{12}$$

$$P_{\mathrm{sw,IGBT}}(D, T_{\mathrm{j}}, I) = f_{\mathrm{sw}}\cdot E_{\mathrm{on+off}}(T_{\mathrm{j}})\cdot\left(\frac{I_{\mathrm{DC,avg}}}{I_{\mathrm{ref}}}\right)^{k_{\mathrm{iT}}}\cdot\left(\frac{V_{\mathrm{DC}}}{V_{\mathrm{ref}}}\right)^{k_{\mathrm{vT}}}\cdot(1 + TC_{\mathrm{Esw}}\cdot\Delta T) \tag{13}$$

with $\Delta T = (T_{\mathrm{j}} - T_{\mathrm{ref}})$. The relevant coefficients for the voltage and current dependencies ($k_{\mathrm{iD}}, k_{\mathrm{vD}}, k_{\mathrm{iT}}, k_{\mathrm{iT}}$) can be taken from [13]. The DRBC has an inductance, which causes additional losses. Here, the iron losses are only considered. They are dependent on the resistance that is considered to be $0.02\ \Omega$, which is a typical value for a boost converter inductance [18].

$$P_{Ind}(I) = R_L I^2_{\mathrm{DC,avg}} \tag{14}$$

As it can be seen in the equations, the losses are mainly dependent on the current through an element. These currents are proportional to the generator voltage, that is influenced by the wind speed. Altogether, the inductance, switching and conduction losses of the DRBC are added as it can be seen in eq. 15.

$$P_{\mathrm{L,DRBC}}(D, T_{\mathrm{j}}, I) = P_{\mathrm{DR}}(T_{\mathrm{j}}) + P_{\mathrm{cond}}(D, T_{\mathrm{j}}, I) + P_{\mathrm{sw}}(D, T_{\mathrm{j}}, I) + P_{\mathrm{L}}(I) \tag{15}$$

3.4 Diode Rectifier with a switch mode rectifier

The DRSMR has the same behavior as the DRBC. The only difference is the non existing inductance in the DC-link [4, 5]. The currents and voltages have the same shapes. Consequently, the losses are:

$$P_{\mathrm{L,DRSMR}}(D, T_{\mathrm{j}}, I) = P_{\mathrm{DR}}(T_{\mathrm{j}}) + P_{\mathrm{cond}}(D, T_{\mathrm{j}}, I) + P_{\mathrm{sw}}(D, T_{\mathrm{j}}, I). \tag{16}$$

3.5 Half bridge switch mode rectifier

The currents through the semiconductors are depicted in fig. 4. As it can be seen the waveforms are comparable to the current of the DR, but they are additional influenced by the duty cycle. For the diode and IGBT, the following current functions are assumed:

$$i_{\mathrm{F,upperD}}\,(\omega t, D) = i_{\mathrm{DR}}\,(\omega t, V_{\mathrm{DC,HSS}}, D) \tag{17}$$

$$i_{\mathrm{F,antiD}}\,(\omega t, D) = i_{\mathrm{DR}}\,(\omega t, V_{\mathrm{DC,HSS}}) \tag{18}$$

$$i_{\mathrm{c}}\,(\omega t, D) = i_{\mathrm{DR}}\,(\omega t, V_{\mathrm{DC,HSS}}, D) \tag{19}$$

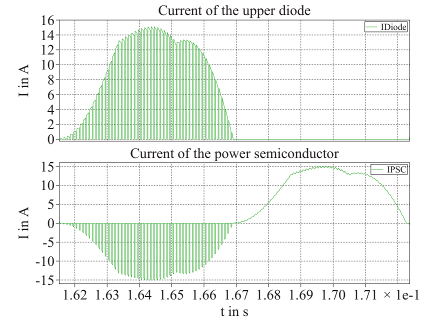

Fig. 4: Current in a phase of the half bridge switch mode rectifier

With the eq. (1)-(3) and eq. (**??**)-(19), the conduction and switching losses P_{cond} and P_{sw} are:

$$P_{\text{cond,upperD}}(D, T_j, I) = \frac{1}{2} \cdot (1 - D) \cdot V_{\text{F0}} \cdot I_{\text{GR,bar}} + \frac{1}{2} \cdot (1 - D) \cdot (r_{\text{F},25^\circ\text{C}} + TC_r \cdot \Delta T) \cdot I^2_{\text{GR,RMS}} \tag{20}$$

$$P_{\text{cond,antiD}}(D, T_j, I) = \frac{1}{2} \cdot V_{\text{F0}} \cdot I_{\text{GR,bar}} + \frac{1}{2} \cdot (r_{\text{F},25^\circ\text{C}} + TC_r \cdot \Delta T) \cdot I^2_{\text{GR,RMS}} \tag{21}$$

$$P_{\text{cond,IGBT}}(D, T_j, I) = \frac{D}{2} \cdot V_{\text{CE0}} \cdot I_{\text{GR,bar}} + \frac{a}{2} \cdot r_{\text{CE}} \cdot I^2_{\text{GR,RMS}} \tag{22}$$

$$P_{\text{sw,upperD}}(D, T_j, I) = f_{\text{sw}} \cdot (E_{\text{rr}}) \cdot \left(\frac{I_{\text{GR,avg}} \cdot (1 - D)}{I_{\text{ref}}} \right)^{K_{\text{iD}}} \cdot \left(\frac{V_{\text{DC}}}{V_{\text{ref}}} \right)^{K_{\text{vD}}} \cdot (1 + TC_{\text{Err}} \cdot \Delta T) \tag{23}$$

$$P_{\text{sw,antiD}}(D, T_j, I) = f_{\text{sw}} \cdot (E_{\text{rr}}) \cdot \left(\frac{I_{\text{GR,avg}}}{I_{\text{ref}}} \right)^{K_{\text{iD}}} \cdot \left(\frac{V_{\text{DC}}}{V_{\text{ref}}} \right)^{K_{\text{vD}}} \cdot (1 + TC_{\text{Err}} \cdot \Delta T) \tag{24}$$

$$P_{\text{sw,IGBT}}(D, T_j, I) = f_{\text{sw}} \cdot (E_{\text{on}} + E_{\text{off}}) \cdot \left(\frac{D \cdot I_{\text{GR,avg}}}{I_{\text{ref}}} \right)^{K_{\text{i}}} \cdot \left(\frac{V_{\text{DC}}}{V_{\text{ref}}} \right)^{K_{\text{v}}} \cdot (1 + TC_{\text{Esw}} \cdot \Delta T) \tag{25}$$

Again, the losses are dependent on the current, which are influenced by the generator voltage, that is proportional to the wind speed. The overall losses of the HSMR is the sum of the conduction and switching losses for the three phases:

$$P_{\text{HSMR}}(D, T_j, I) = 3 \cdot \left(P_{\text{cond}}(D, T_j, I) + P_{\text{sw}}(D, T_j, I) \right) \tag{26}$$

3.6 Two Level Converter

The generator phase currents are assumed to be sinusoidal. For the RMS calculation, the harmonics are neglected. The RMS value of a sinusoidal signal is: $I_{\text{gen,RMS}} = \frac{1}{\sqrt{2}} \cdot \hat{I}_{\text{gen}}$. The current functions of the 2LC are given in [13]. The overall losses are again the sum of the switching and conduction losses.

3.7 Machine losses

The machine losses consist of different losses like windage, friction, core, stray load, and copper losses [18]. Here, only the iron and copper losses of the stator are considered in the loss calculation. The iron losses are composed of hysteresis and stray losses. There are different possibilities to calculate the machine losses [19, 20], but here, the focus is on the influence of the rectifiers. The loss calculation is therefore based on the generator currents and the approach of [21] will be briefly described.
The losses are depended on material constants, the angular frequency of the applied voltage and the harmonics of the flux density. The armature reaction field of a SPMSM is assumed to be sinusoidal.The harmonics of the flux density are dependent on the harmonics of the current as well as some machine constants, which will be assumed to be the same for all rectifiers. In sum the iron losses are dependent on certain machine parameters, which are summarized in the factors K_{em} and K_{hm}, and on the harmonics of the currents [21]:

$$P_{\text{Fe}} = K_{\text{em}} \sum_n \left(\omega_{gen} \right)^2 I_n^2 + K_{\text{hm}} \sum_n \left(\omega_{gen} \right) I_n^2. \tag{27}$$

As it can be seen in Eq. (27), the losses are depended on the fundamental and the harmonics of the phase currents. The harmonics are in general calculated by the subtraction of the RMS value and the fundamental of the current:

$$\sum_n I_{\mathrm{n}}^2 = I_{\mathrm{RMS}}^2 - I_1^2. \tag{28}$$

4 Results

For simulating the losses of the five different rectifier topologies, a thermal model with the data shown in tab. 2 is built. The grid side inverter is neglected and modeled with a DC voltage source with a constant amplitude. The input torque is generated by a wind turbine model described in [22]. In general, the generated power is dependent on the wind speed. For a wind turbine with a power factor of 0.4, a radius of 1.4 m and a tip speed ration of 8, the power curves for each topology can be seen in Fig. 5. As it can

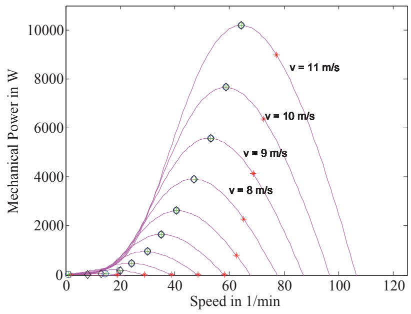

Fig. 5: Mechanical power on dependency on the wind speed for each topology: Red: DR, green: DRBC, cyan: DRSMR, blue: HSMR, black: 2LC

be seen, for different wind speeds different powers are generated. For comparing the losses for the five topologies, the mechanical power is the scaling factor for the losses. That means, the losses are related to the mechanical power:

$$Loss\ ratio = \frac{P_{\mathrm{L}}(v)}{P_{\mathrm{mech}}(v)}. \tag{29}$$

The losses related to the mechanical power for each wind speed is depicted in fig. 6. In Fig. 6 a) the power semiconductor losses of the rectifiers related to the mechanical power are shown. Generally, the loss ratio decreases with an increasing wind speed. That can be explained with the increasing mechanical power which is proportional to the wind speed up to three ($P_{\mathrm{v}} = \frac{1}{2}\rho A v^3$). As it can be seen from the red line, the losses of the DR are low. But at smaller wind speeds, the DR does not generate energy out of the wind. The highest losses are generated from the boost converter. Besides the power semiconductors, the inductance causes additional losses. For higher wind speeds, the losses vs. the generated mechanical power are lower.

The machine losses related to the mechanical power are depicted in fig. 6 b). Here, the machine constants are supposed to be similar. First, the losses grow due to the increasing speed of the system. At a certain point, the harmonics of the system are decreasing and hence the losses become smaller as well.

In fig. 6 c) the total losses are shown. The machine losses are the dominant losses. Consequently, the DR has the highest losses followed by the DRBC and DRSMR.

5 Discussion

The losses related to the mechanical power of the rectifiers are decreasing for higher wind speeds. The diodes have low losses compared to the power semiconductors. With a high blocking voltage and high mean current, the power semiconductor of the DRBC (green) and DRSMR (pink) generate the highest losses. Consequently, these two topologies have the highest losses compared to the other topologies. The DRBC has the overall highest losses due to the additional inductance. The 2LC (black) has beside the DR (red) the lowest losses. The HSMR (blue) has the third lowest losses.

The machine losses are shown for a material constant of $K_{\mathrm{em}} = 0.05$ and $K_{\mathrm{hm}} = 0.05$. For the comparison of the rectifiers it is considered that the constants are the same for each rectifier. Within the variation of the machine constants, the losses will vary as well. But comparing the losses for each rectifier, the

ISBN 978-3-8007-3924-0

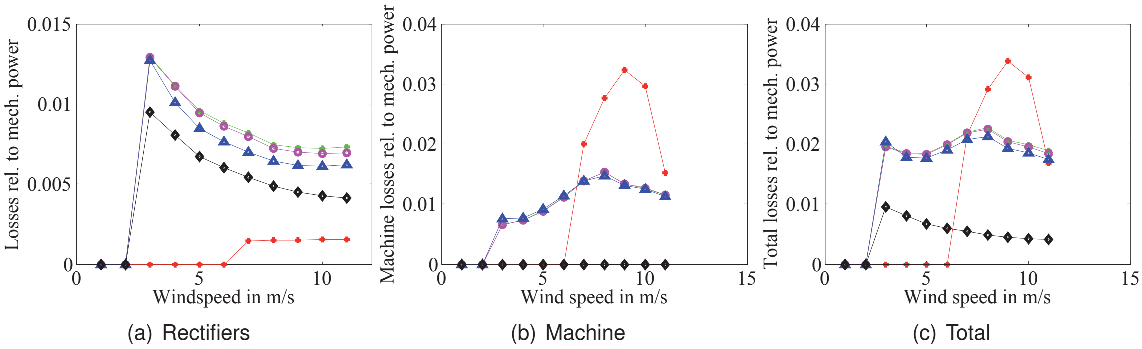

Fig. 6: Simulated losses related to the generated mechanical power: Red: DR, green: DRBC, pink: DRSMR, blue: HSMR, black: 2LC

proportion will be similar. That means these results are valid for comparing the rectifiers. As a result, in can be concluded, that the machine losses decrease for higher wind speeds, since the harmonics are reduced. The DR has the highest losses, whereas the 2LC has the lowest machine losses. For the design of the generator, the shape of the currents and therefore the reaction to the machine is not negligible. With higher harmonics and losses, the generator has to have a higher inductance, which is realized with a higher number of pole pairs. This has consequences concerning the costs and the volume of the generator. The advantage of the 2LC is therefore, that the machine inductance can be reduced compared to the other topologies.

6 Conclusion

In this paper the losses of different rectifiers used in a SWT system and its impact on the shape of the phase currents in dependency on the wind speed are analyzed. The DR produces the lowest losses but in contrast it is not able the generate a power at low wind speeds. For a wind region with high wind speed the DR is a topology which provides low rectifier losses. If the machine is considered as well, the losses of the DR are higher. As it can be seen, the losses of the machine are different concerning different rectifiers. With higher distortion of the current, the losses of the machine increase which has to be considered in the design of the machine. For higher wind speeds, the losses related to the mechanical power decrease. For an optimal drive train, the wind speed profiles have to be considered.

7 Acknowledgment

The authors give their sincere thanks to EKSH (Cooperation for Energy and Climate Protection - Schleswig-Holstein) for funding this research project.

References

[1] Caliskan, V., Perreault, D.J., Jahns, T.M., and Kassakian, J.G.: *Analysis of three-phase rectifiers with constant-voltage loads*. Circuits and Systems I: Fundamental Theory and Applications, IEEE Transactions on, 50(9):1220–1225, Sept. 2003.

[2] Pejovic, P. and Kolar, J.W.: *An analysis of three-phase rectifiers with constant voltage loads*. In *Circuits and Systems for Communications (ECCSC), 5th European Conference on*, pages 119–126, Nov. 2010.

[3] Ivanovic, Z., Blanusa, B., and Knezic, M.: *Algorithm for efficiency optimization of the boost converter in wind turbine*. In *Power Electronics and Motion Control (EPE/PEMC), 15th International Conference on*, pages DS3c. 9–1 – DS3c.9–6, 2012.

[4] Pathmanathan, M., Soong, W.L., and Ertugrul, N.: *Output power capability of surface pm generators with switched-mode rectifiers*. In *Sustainable Energy Technologies (ICSET), IEEE International Conference on*, pages 1–6, 2010.

[5] Whaley, D.M., Soong, W.L., and Ertugrul, N.: *Investigation of switched-mode rectifier for control of small-scale wind turbines*. In *Industry Applications, 40th IAS Annual Meeting. Conference Record of the*, volume 4, pages 2849 – 2856, Oct. 2005.

[6] Oliveira, D.S., Reis, M.M., Silva, C. E A, Colado Barreto, L., Antunes, F. L M, and Soares, B.L.: *A three-phase high-frequency semicontrolled rectifier for pm wecs*. Power Electronics, IEEE Transactions on, 25(3):677–685, 2010.

[7] Chen, Lujie, Soong, W.L., Pathmanathan, M., and Ertugrul, N.: *Comparison of ac/dc converters and the principles of a new control strategy in small-scale wind turbine systems*. In *Universities Power Engineering (AUPEC), 22nd Australasian Conference on*, pages 1–6, 2012.

[8] Reis, M.M., Soares, B., Barreto, L. H S C, Freitas, E., Silva, C. E A, Bascope, R.T., and Oliveira, D.S.: *A variable speed wind energy conversion system connected to the grid for small wind generator*. In *Applied Power Electronics and Exposition (APEC), 23rd Annual IEEE Conference on*, pages 751–755, 2008.

[9] Buchert, K. and Fuchs, F.W.: *Comparison of three phase rectifier topologies in small wind turbines*. In *16th Conference on Power Electronics and Applications, EPE' 14-ECCE Europe*, 2014.

[10] Pathmanathan, M., Tang, C., Soong, W.L., and Ertugrul, N.: *Comparison of power converters for small-scale wind turbine operation*. In *Universities Power Engineering (AUPEC), 18th Australasian Conference on*, pages 1 – 6, Dec. 2008.

[11] Kortabarria, Inigo, Ibarra, Edorta, Alegria, Inigo Martinez de, Andreu, Jon, and Ascarza, Ainhoa: *Power converters used in grid connected small wind turbines: Analysis of alternatives*. In *Power Electronics, Machines and Drives (PEMD), 5th IET International Conference on*, pages 1 – 6, April 2010.

[12] Graovac, D. and Pürschel, M.: *AN: IGBT Power Losses Calculation Using the Data-Sheet Parameters*. Infineon AG, Jan. 2009.

[13] Wintrich, A., Nicolai, U., Tursky, W., and Reimann, T.: *Application Manual Power Semiconductors*. SEMIKRON International GmbH, 2010.

[14] Mohan, Ned, Undeland, Tore M., and Robbins, William P.: *Power Electronics: Converters, Applications, and Design*. Wiley, 2nd edition, January 1995. http://amazon.com/o/ASIN/0471584088/.

[15] Pejovic, P. and Kolar, J.W.: *Exact analysis of three-phase rectifiers with constant voltage loads*. Circuits and Systems II: Express Briefs, IEEE Transactions on, 55(8):743–747, Aug. 2008.

[16] Boldea, Ion: *Variable Speed Generators (The Electric Generators Handbook)*. CRC Press, 1st edition, Nov. 2005.

[17] Bronstein, I.N., Semendjajew, K.A., Musiol, G., and Mühlig, H.: *Handbook of mathematics*, volume 6. Verlag Harri Deutsch, 2005, ISBN 3-8171-2006-0.

[18] Almeida, A.T. de, Ferreira, F.J.T.E., and Fong, J.A.C.: *Standards for efficiency of electric motors*. Industry Applications Magazine, IEEE, 17(1):12–19, Jan. 2011.

[19] Tamura, J.: *Calculation method of losses and efficiency of wind generators*. In Muyeen, S.M. (editor): *Wind Energy Conversion Systems*, Green Energy and Technology, pages 25–51. Springer London, 2012.

[20] Nguyen, T.D., Tseng, K.J., Zhang, C., and Zhang, S.: *Loss study of a novel axial flux permanent magnet machine*. In *Electric Machines Drives (IEMDC), IEEE International Conference on*, pages 1143–1148, May 2011.

[21] Hassan, W. and Wang, B.: *Efficiency optimization of pmsm based drive system*. In *Power Electronics and Motion Control (IPEMC), 7th International Conference on*, volume 2, pages 1027–1033, June 2012.

[22] Jayalakshmi, N.S., Gaonkar, D.N., and Kumar, K.S.K.: *Dynamic modeling and performance analysis of grid connected pmsg based variable speed wind turbines with simple power conditioning system*. In *Power Electronics, Drives and Energy Systems (PEDES), IEEE International Conference on*, pages 1–5, 2012.